Dariusz CZERWIŃSKI, Ryszard GOLEMAN

Lublin University of Technology, Faculty of Electrical Engineering and Computer Science

doi:10.15199/48.2016.06.20

Lumped parameter thermal model of the rectangular bar in an induction motor rotor

***Abstract**. The paper proposes a temperature model with lumped parameters for the rectangular winding bar of a cage induction motor using Coselica toolbox in Scilab software. An analysis of the cage bar's heating during a standstill of the motor was carried out. It took into consideration the heat transfer through the package of teeth for different thicknesses of the air gap between the bar and the sheet package.*

***Streszczenie.** W pracy zaproponowano model temperaturowy o parametrach skupionych dla prostokątnego pręta uzwojenia klatkowego silnika indukcyjnego z wykorzystaniem biblioteki Coselica w aplikacji Scilab. Przeprowadzono analizę nagrzewania się pręta klatki w stanie zwarcia silnika. Uwzględniono przejmowanie ciepła przez pakiet zębów dla różnych grubości szczeliny powietrznej pomiędzy prętem a pakietem blach. (**Obwodowy model cieplny prostokątnego żłobka wirnika silnika indukcyjnego**).*

Keywords: deep-bar induction motor, thermal circuit modelling, Coselica, Scilab.
Słowa kluczowe: silnik głębokożłobkowy, obwodowy model cieplny, Coselica, Scilab.

Introduction

The electrodynamic and thermal interactions in the windings of cage induction motors are due to the current flow in the bars of the cage. Especially in the case of high-power electric motors, the analysis of these phenomena is important at the design stage in ensuring the requirements of motors during long start-up and increasing their durability [1-5].

The heating analysis of the bars in the motor's cage at standstill indicates a fast rise of temperature in the region of the bars, which leads to an increase in mechanical stress in the cage [1,2,6-10]. The temperature distribution in the bar depends on the efficiency of heat transfer by the teeth of the rotor, which is conditioned by the width of the technological air gap existing between the bar and the sheet package, as well the effectiveness of the heat transfer to the motor's air gap.

Temperature field analysis can be done mathematically with partial differential equations or by using numerical methods [11]. Analytical methods are difficult to apply due to the geometry and nonlinearity of the physical properties of the materials. In numerical methods the FEM, BEM and equivalent thermal circuits can be distinguished. However, there is a need to use dedicated software or write one's own. Commercial analysis packages which can be used, are: FLUX, Comsol Multiphysics, ANSYS, OPERA, QuickField and Matlab. In Open Source or free packages FEMM, LISA, Elmer and Scilab/Xcos can be listed. In the case when the temperature distribution in the whole model is not required, an equivalent circuit model of heat transfer can be used.

In a lumped parameter thermal model the structure of the model is simplified and the results of the transient analysis are obtained much faster [12].

Circuit model of deep slot

In the motor standstill condition the transient analysis was made of the rectangular bar heating with a heat transfer in the air gap and the rotor package teeth. The simplified geometry of the rotor slot is shown in Fig. 1.

The deep slot was modelled as the second order circuit thermal model. The copper cage and iron teeth were presented as heat capacitor elements. In the copper cage the alternating component of stalling current is equal to 7955 A.

This current generates the heat, which is represented by the fixed heat flow element in the model named Cu_bar shown in Figure 2.

The iron parts of the rotor are connected through the thermal conductance Rp_right shown in Figure 3, which represents the air gap. Uncovered parts of the rotor are cooled with air, assuming the free convection condition. In the standstill conditions there is no forced air flow around the rotor. The convection is represented by the Cu_air_conv and Fe_air_conv elements shown in Figures 2 and 3.

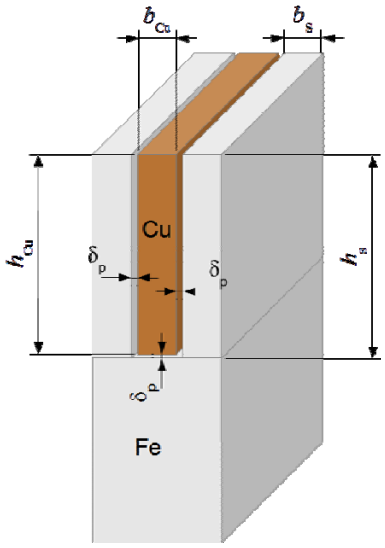

Fig. 1. Simplified geometry of the rotor slot of an induction motor

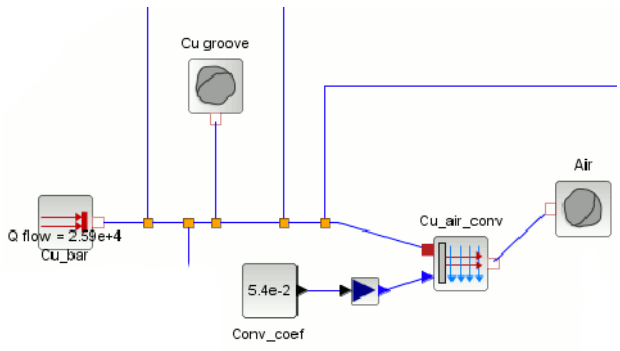

Fig. 2. Part of the model representing the copper cage bar (Cu_groove) and heat source (Cu_bar)

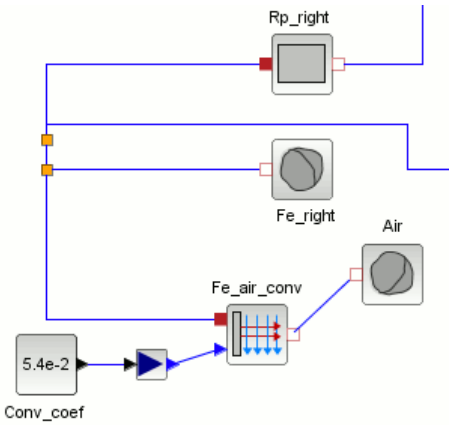

Fig. 3. Fragment of the model representing the iron part of the rotor

The basic equation for heat convection between the solid and fluid is:

(1) $$Q_{conv} = G_c \cdot (T_{solid} - T_{fluid})$$

where: T_{solid}, T_{fluid} – respective temperatures of solid and fluid, G_c – an input signal to the components Cu_air_conv and Fe_air_conv, which depends on the cooling conditions.

G_c may be calculated according to:

(2) $$G_c = A \cdot h$$

where: A – convection area, h – heat transfer coefficient

The heat transfer coefficient h is calculated from the properties of the fluid flowing over the solid. In the case of a standstill of an induction motor the rotor is not moving and free convection is assumed.

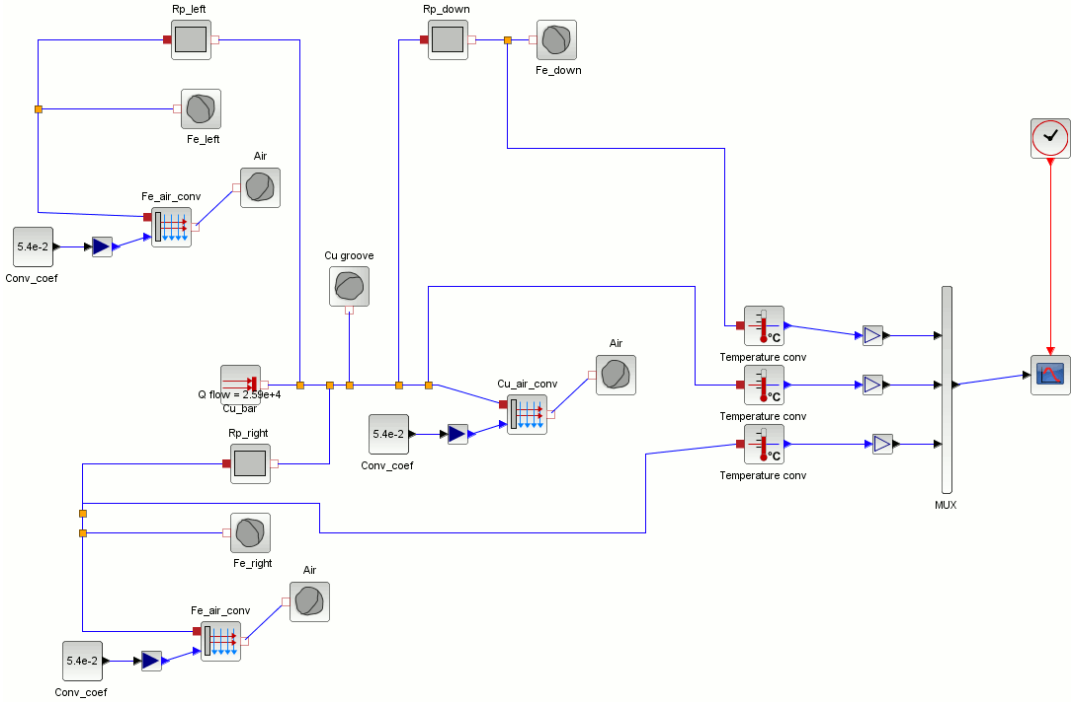

Fig. 4. Circuit thermal model of the deep bar

In that case the heat transfer coefficient is constant and equal to:

(3) $$h = 12 \frac{\mathrm{W}}{\mathrm{m^2K}}$$

The above assumptions allow to build a thermal circuit model of the deep slot. The model was built in a Scilab/Xcos environment, which is an OpenSource clone of Matlab. Additionally in an Xcos environment the Coselica toolbox was installed, implementing the circuit thermal blocks.

The model, consisting of additional elements of the slot as well as temperature sensors is shown in Figure 4. It allows to solve the nonlinear transient heat equations. The results permit to determine the temperature changes in time in the Cu deep bar of the motor (middle temperature sensor in Figure 4). The temperature changes over time are shown in Figure 5. It can be seen that the temperature of the Cu bar rises from 20 °C to about 750 °C during standstill.

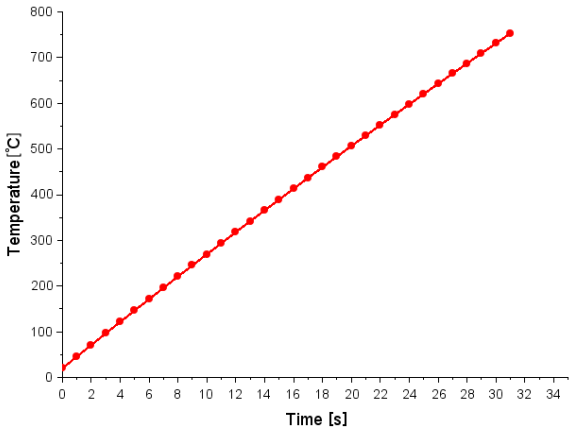

Fig. 5. Temperature of the deep bar versus time during standstill

The maximum value is close to that obtained analytically in [4] (about 720 °C), however there is no information on the temperature distribution along the height of the copper bar.

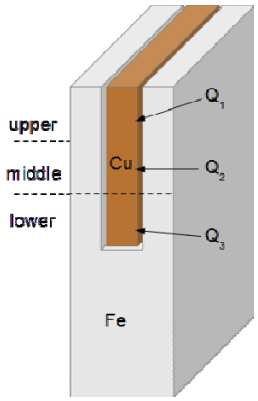

Fig. 6. Simplified geometry of the rotor slot with modified model sections marked

To overcome this limitation the modified model of deep groove was introduced. The copper bar and iron slot were divided into three parts shown in Figure 6. The copper bar was partitioned into three equal parts. In each part the heat sources, caused by the standstill current, were assumed (Q_1-Q_3). The iron part of the groove was modelled analogously, although the lower part was created with a higher value of heat capacitance due to the larger volume of the middle rotor part.

The dimensions of the simplified model of the rotor slot and square bar are given in Table 1.

Table 1. Dimensions of simplified model of the rotor slot and square bar

h_s	$h_{Cu}= h_s-\delta_p$	b_{Cu}	b_s	δ_p
mm	mm	mm	mm	mm
62	61.75 61.9	4.5	4.5	0.25 0.1

The modified model was introduced in a Scilab/Xcos environment and is shown in Figure 7.

The model consists of 3 layers, which are represented by thermal circuit elements analogous to the simplified model. The connection between the copper parts of the bar was modelled as thermal conductance, with its value calculated from Equation (4)

$$G_{Cu} = \frac{\lambda \cdot A}{l} \tag{4}$$

where: A – vertical cross-section of the bar, l – 1/3 of bar height h_{Cu}, λ – specific thermal conductivity of copper.

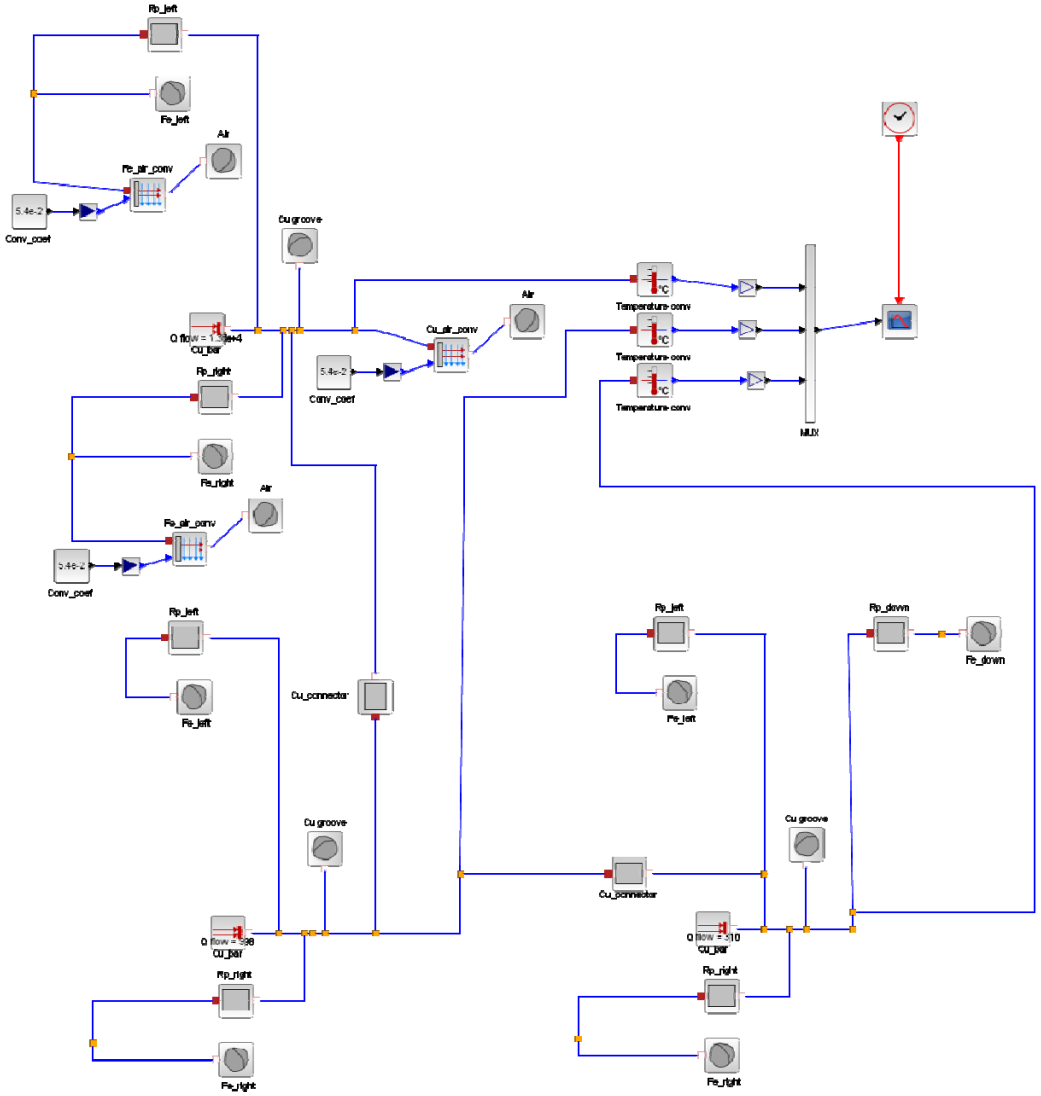

Fig. 7. Modified 3-layer circuit thermal model of the rectangular bar

Due to the three layers of the modified model introducing the thermal conductance of copper was necessary for proper circuit connections. This approach is based on Beuken's models and is also used in other works

[13]. It can also be noticed that there is no direct vertical connection between the iron thermal capacitances. The total value of iron and air capacitances is much higher compared to copper, and assuming the simplicity of the model, vertical connections were neglected.

The properties of the materials used during calculations are shown in Table 2.

Table 2. The materials' constants and coefficients used in the calculations

Property	Value
specific thermal conductivity of copper	λ_m = 372 W/m·K
specific thermal conductivity of laminated core	λ_z = 56 W/m·K
effective thermal conductivity of the air gap	λ_p = 0,03 W/m·K
specific heat of copper	c_m = 419 W·s/kg·K
specific heat of laminated core	c_z = 461 W·s/kg·K
heat transfer coefficient of copper	α_{Cu} = 30 W/m^2·K
heat transfer coefficient of laminated core	α_z = 20 W/m^2·K
density of copper	ρ_{Cu} = 8900kg/m^3
density of laminated core	ρ_z = 7900kg/m^3
volumetric magnetic losses in the tooth	q_z = 0,17 W/m^3

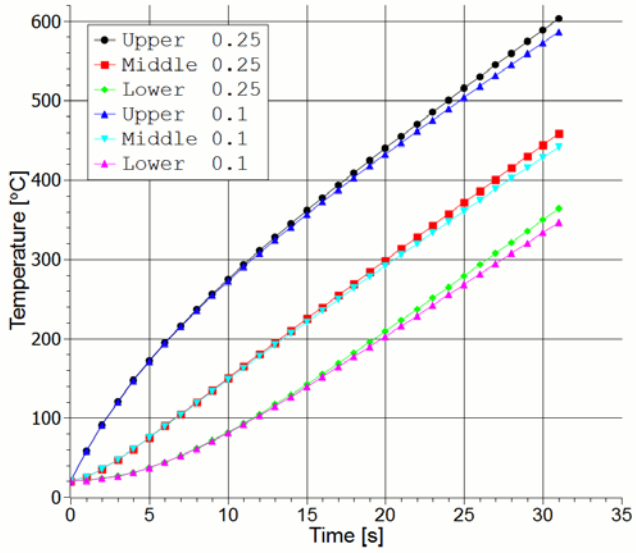

Fig. 8. Simplified geometry of the rotor slot with modified model sections marked

The temperature changes over time in parts of the Cu deep bar of the motor (temperature sensors in Figure 7) were determined and are shown in Figure 8. Decreasing the equivalent air gap (2.5 times) causes the changes in temperature distribution. The final temperature value is lower in the case of a smaller air gap and this value is equal in corresponding layers (upper, middle, lower) to 586°C, 441°C and 346°C, respectively.

Conclusions

In the standstill and the initial start-up phase of the induction motor there is a significant temperature increase in the bars of the cage.

The unequal temperature distribution in the bars causes mechanical stress in the cage and reduces its durability.

The circuit model allows to implement the heat calculations in the case of the deep slot of an induction motor at standstill (in the short circuit conditions).

It is possible to calculate the changes of the temperature over time in individual parts of the groove.

An equivalent air gap between the bar and the package of teeth affects the degree of heat transfer by the package.

Matching the bar and the groove causes the decrease in temperature of the rectangular bar of an induction motor.

The model takes into account the heat transfer through the air gap and the packet teeth of the rotor. It may be useful for the design and performance of cage windings. Because of its simplicity and accessibility of the Scilab/Xcos environment it can be widely used.

***Authors**: dr hab inż. Dariusz Czerwiński, prof. nadzw., e-mail: d.czerwinski@pollub.pl, dr hab. inż. Ryszard Goleman, prof. nadzw., e-mail: r.goleman@pollub.pl; Lublin University of Technology, Faculty of Electrical Engineering and Computer Science, ul. Nadbystrzycka 38A, 20-618 Lublin*

REFERENCES

[1] Pliś D., Płoszyńska J., The effect of relative magnetic permeability of wedges closing stator slots in a cage induction motor on rotor cage heating during the starting phase, Przegląd Elektrotechniczny, 88 (2012), nr 12b, 89-92.

[2] Rut R., Wpływ przejmowania ciepła przez rdzeń wirnika na szybkość narastania temperatury w głębokożłobkowych prostokątnych prętach uzwojenia klatkowego silnika indukcyjnego, Rozprawy Elektrotechniczne, 33 (1987), z. 3-4, 787-797.

[3] Williamson S.; Lloyd M.R., Cage rotor heating at standstill, IEE Proceedings B, Electric Power Applications, 1987, vol. 134, Issue: 6, pp: 325-332.

[4] Xyptras, J.; Hatziathanassiou, V., Thermal analysis of an electrical machine taking into account the iron losses and the deep-bar effect, IEEE Transactions on Energy Conversion, 1999, vol. 14, Issue: 4, pp: 996-1003.

[5] Feyzi, M.R.; Parker, A.M., Heating in deep-bar rotor cages, Electric Power Applications, Electric Power Applications, IEE Proceedings, 1997, vol. 144, issue: 4, pp: 271-276.

[6] Weili Li, Junci Cao, Xiaochen Zhang, Electrothermal Analysis of Induction Motor With Compound Cage Rotor Used for PHEV, IEEE Transactions on Industrial Electronics, 2010, vol. 57, Issue: 2, pp: 660-668.

[7] Walker, J.D.; Williamson, S., Temperature rise in induction motors under stall conditions, IEEE Colloquium on Thermal Aspects of Machines, 1992, pp: 7/1-7/4.

[8] Siyambalapitiya, D.J.T.; McLaren, P.G.; Tavner, P.J., Transient thermal characteristics of induction machine rotor cage, IEEE Transactions on Energy Conversion, 1988, vol. 3, Issue: 4, pp: 849-854.

[9] Williamson, S.; Walker, J.D., Calculation of stall bar temperature rise, Fifth International Conference on (Conf. Publ. No. 341) Electrical Machines and Drives, 1991, pp: 271-275.

[10] Cao Junci; Li Weili; Huo Feiyang; Cheng Peng; Sheng Jiafeng, The heat conducting analysis of transient temperature field in IMCCR with discontinuous blocked rotor under different structure, EUROCON 2009, EUROCON '09. IEEE, 2009, pp: 696-702.

[11] Lienhard IV J.,H., Lienhard V J.,H., A heat transfer textbook, Third Edition, Cambridge, Massachusetts, U.S.A., 2001.

[12] Campo A., On the teaching of the lumped model for unsteady heat conduction; natural convection versus forced convection, Latian American and Caribbean Journal of Engineering Education, Vol 5(2), 2010, 1-5.

[13] Wesołowski M., Mikułowicz B., Skrzypczak P., Hauser J., The work stand based on Beuken model for temperature controllers testing, Academic Journals, Poznań University of Technology, No. 84, 2015, pp: 93-102.